Inorg. Chem. **2005**, *44*, 2628–2638

Facile Synthesis, Structure, and Luminescence Properties of Pt(diimine)bis(arylacetylide) Chromophore–Donor Dyads

Thaddeus J. Wadas, Soma Chakraborty, Rene J. Lachicotte, Quan-Ming Wang, and Richard Eisenberg*

Department of Chemistry, University of Rochester, Rochester, New York 14627

Received August 13, 2004

The luminescent complex Pt(dpphen)bis(arylacetylide) complex (**1**) (dpphen = 4,7-diphenylphenanthroline and arylacetylide = 4-ethynylbenzaldehyde) has been synthesized and characterized structurally and spectroscopically. Complex **1** has been employed in the synthesis of donor–chromophore (D–C) dyads through Schiff base condensations of different anilines to give imine-linked dyads **2**–**4** and through imine reduction with borohydride, to give the corresponding amine-linked dyads **2a**–**4a**. Crystal structure determinations of **1**–**4** and **4a** establish a distorted square-planar geometry around the Pt(II) ion in each system with cis arylacetylide ligands and a diimine-constrained N–Pt–N bond angle of ca. 79.5°. Complex **1** is strongly emissive having a relative quantum yield (ϕ) of 36% and an excited-state lifetime of 3.1 μs. In accord with the notion of photoinduced electron transfer from the aniline-based donor to the photoexcited chromophore, the emission of dyads **2**–**4** and **2a**–**4a** is effectively quenched in all solvents tested. The intense absorption at 400 nm (30000–70000 L/mol·cm) for **2** and **2a** has been assigned as an intraligand π–π* transition, whereas the lowest-energy transitions for all other dyads correspond to Pt-to-π*(diimine) MLCT transitions. Although the dyads can be synthesized in a facile manner, photolysis experiments reveal that both the imine and amine linkages are photochemically unstable, resulting in hydrolysis and regeneration of the aldehyde-containing chromophore **1**.

Introduction

Photosynthesis involves the conversion of light energy into chemical potential energy and is accomplished through a series of events including photon capture, electron−hole pair creation, charge separation, charge accumulation, and catalysis of the energy-storing reaction.[1−17] Over the past two decades, efforts in the development of artificial photosynthetic systems have included the design, synthesis and study of two- and three-component systems (dyads and triads) for photoinduced charge separation.[11,15,18−25] In these investigations, the photochemically active component is generally a transition metal chromophore with a d^6 metal ion [primarily Ru(II), Os(II), and Re(I)] and an unsaturated diimine ligand for charge-transfer excitation. The other components in these

* Author to whom correspondence should be addressed. Email: eisenberg@chem.rochester.edu.

(1) Balzani, V.; Moggi, L.; Scandola, F. Towards a Supramolecular Photochemistry: Assembly of Molecular Components to Obtain Photochemical Molecular Devices. In *Supramolecular Photochemistry*; Balzani, V., Ed.; D. Reidel Publishing Co.: Dordrecht, The Netherlands, 1987; pp 1−28.
(2) Wasielewski, M. R. *Chem. Rev.* **1992**, *92*, 435−461.
(3) Yonemoto, E. H.; Saupe, G. B.; Schmehl, R. H.; Hubig, S. M.; Riley, R. L.; Iverson, B. L.; Mallouk, T. E. *J. Am. Chem. Soc.* **1994**, *116*, 4786−4795.
(4) Kroon, J.; Verhoeven, J. W.; Paddon-Row, M. N.; Oliver, A. M. *Angew. Chem., Int. Ed. Engl.* **1991**, *30*, 1358−1360.
(5) Cusack, L.; Marguerettaz, X.; Rao, S. N.; Wenger, J.; Fitzmaurice, D. *Chem. Mater.* **1997**, *9*, 1765−1772.
(6) Osuka, A.; Nakajima, S.; Okada, T.; Taniguchi, S.; Nozaki, K.; Ohno, T.; Yamazaki, I.; Nishimura, Y.; Mataga, N. *Angew. Chem., Int. Ed. Engl.* **1996**, *35*, 92−95.
(7) Moore, A. L.; Moore, T. A.; Gust, D.; Silber, J. J.; Sereno, L.; Fungo, F.; Otero, L.; SteinbergYfrach, G.; Liddell, P. A.; Hung, S. C.; Imahori, H.; Cardoso, S.; Tatman, D.; Macpherson, A. N. *Pure Appl. Chem.* **1997**, *69* (10), 2111−2116.
(8) Gust, D.; Moore, T. A.; Makings, L. R.; Liddell, P. A.; Nemeth, G. A.; Moore, A. L. *J. Am. Chem. Soc.* **1986**, *108*, 8028−8031.
(9) Gust, D.; Moore, T. A.; Moore, A. L. *Acc. Chem. Res.* **2001**, *34*, 40−48.
(10) Imahori, H.; Cardoso, S.; Tatman, D.; Lin, S.; Noss, L.; Seely, G. R.; Sereno, L.; deSilber, J. C.; Moore, T. A.; Moore, A. L.; Gust, D. *Photochem. Photobiol.* **1995**, *62* (6), 1009−1014.
(11) Ziessel, R.; Juris, A.; Venturi, M. *Inorg. Chem.* **1998**, *37* (20), 5061−5069.
(12) Dixon, I. M.; Collin, J. P.; Sauvage, J. P.; Barigelletti, F.; Flamigni, L. *Angew. Chem., Int. Ed.* **2000**, *39*, 1292.
(13) Meyer, T. J. *Acc. Chem. Res.* **1989**, *22*, 163−170.
(14) Chan, C.-W.; Lai, T. F.; Che, C.-M.; Peng, S.-M. *J. Am. Chem. Soc.* **1993**, *115* (24), 11245−11253.
(15) Treadway, J. A.; Chen, P. Y.; Rutherford, T. J.; Keene, F. R.; Meyer, T. J. *J. Phys. Chem. A* **1997**, *101* (37), 6824−6826.
(16) Slate, C. A.; Striplin, D. R.; Moss, J. A.; Chen, P. Y.; Erickson, B. W.; Meyer, T. J. *J. Am. Chem. Soc.* **1998**, *120* (19), 4885−4886.

10.1021/ic048886l CCC: $30.25
Published on Web 03/23/2005

systems for charge separation by electron transfer are commonly organic moieties such as phenothiazines and arylamines as donors and fullerenes, porphyrins, and quinones as acceptors.[8,11,26−35]

A different class of chromophores that has been studied by us and others consists of diimine-based square-planar Pt(II) complexes having the general formula Pt(diimine)L_2.[36−40] The diimine in these complexes corresponds to 2,2′-bipyridine, 1,10-phenanthroline, or derivatives thereof. For these chromophores, the LUMO is localized on a π^* orbital of the diimine ligand, and the HOMO has varying extents of metal character influenced by the ancillary ligand L. For systems with L_2 = dithiolate, the HOMO exhibits mixed metal and dithiolate character, whereas for the bis(arylacetylide) complexes (L = C≡CAr), the HOMO is localized on a Pt d orbital.[41−58] The resultant ^{3}MLCT state for the Pt(diimine)bis(acetylide) complexes gives rise to intense luminescence in fluid solution with high emission quantum yields [0.01−0.65 using $Ru(bpy)_3^{2+}$ (ϕ_{em} = 0.062) as a standard] and excited-state lifetimes between 0.1 and 3.0 μs.[38,56,59,60]

Despite the directional charge-transfer excited state of these Pt(II) complexes, only two reports of a Pt(diimine)-bis(acetylide) chromophore being incorporated into dyads or triads currently exist.[40,61] Based on the nature of the excited state in Pt(diimine)$(C{\equiv}CAr)_2$ complexes, the use of these systems as chromophores in dyads and triads requires linkage of the donor to the acetylide ligands and of the acceptor to the diimine. In the first study,[40,61] which focused on the triad shown as **T-I**, phenothiazine served as the one-electron donor, and the nitrophenyl moiety attached via an ethynylidene bridge acted as the acceptor. Cyclic voltammetry of **T-I** detected more facile one-electron oxidation of the phenothiazine donor and reduction of the nitrophenyl group than either process on the chromophore alone. Triad **T-I** was also observed to be nonemissive in fluid solution, and transient absorption studies indicated that rapid charge transfer occurred to generate a charge-separated (CS) state with a 75-ns lifetime in DMF solution. Based on a simple

(17) Imahori, H.; Norieda, H.; Yamada, H.; Nishimura, Y.; Yamazaki, I.; Sakata, Y.; Fukuzumi, S. *J. Am. Chem. Soc.* **2001**, *123*, 100−110.
(18) Danielson, E.; Elliott, C. M.; Merkert, J. W.; Meyer, T. J. *J. Am. Chem. Soc.* **1987**, *109*, 2519−2520.
(19) Lopez, R.; Leiva, A. M. Z. F.; Loeb, B.; Norambuena, E.; Omberg, K. M.; Schoonover, J. R.; Striplin, D.; Devenney, M.; Meyer, T. J. *Inorg. Chem.* **1999**, *38*, 2924−2930.
(20) Bates, W. D.; Chen, P.; Dattelbaum, D. M.; Jones, W. E., Jr.; Meyer, T. J. *J. Phys. Chem. A* **1999**, *103*, 5227−5231.
(21) Harriman, A.; Hissler, M.; Ziessel, R. *Phys. Chem. Chem. Phys.* **1999**, *1* (18), 4203−4211.
(22) Harriman, A.; Odobel, F.; Sauvage, J.-P. *J. Am. Chem. Soc.* **1994**, *116* (12), 5481−5482.
(23) Collin, J.-P.; Guillerez, S.; Sauvage, J.-P.; Barigelletti, F.; De Cola, L.; Flamigni, L.; Balzani, V. *Inorg. Chem.* **1991**, *30*, 4230−4238.
(24) Ballardini, R.; Balzani, V.; Clemente-Leon, M.; Credi, A.; Gandolfi, M. T.; Ishow, E.; Perkins, J.; Stoddart, J. F.; Tseng, H.-R.; Wenger, S. *J. Am. Chem. Soc.* **2002**, *124* (43), 12786−12795.
(25) Hossain, M. D.; Haga, M.; Monjushiro, H.; Gholamkhass, B.; Nozaki, K.; Ohno, T. *Chem. Lett.* **1997**, 573.
(26) Moore, A. N. J.; Katz, E.; Willner, I. *Electroanalysis* **1996**, *8* (12), 1092−1094.
(27) Gust, D.; Moore, T. A.; Moore, A. L.; Lee, S.-J.; Bittersmann, E.; Luttrull, D. K.; Rehms, A. A.; DeGraziano, J. M.; Ma, X. C.; Gao, F.; Belford, R. E.; Trier, T. T. *Science* **1990**, *248*, 199−201.
(28) Gust, D.; Moore, T. A. *J. Photochem.* **1985**, *29*, 173−184.
(29) Seta, P.; Bievenue, E.; Moore, A. L.; Mathis, P.; Bensasson, R. V.; Liddell, P.; Pessiki, P. J.; Joy, A.; Moore, T. A.; Gust, D. *Nature* **1985**, *316*, 653.
(30) Gust, D.; Moore, T. A.; Liddell, P. A.; Nemeth, G. A.; Makings, L. R.; Moore, A. L.; Barrett, D.; Pessiki, P. J.; Bensassori, R. V.; Rougee, M.; Chachaty, C.; DeSchryver, F. C.; Van der Auweraer, M.; Holzwarth, A. R.; Connolly, J. S. *J. Am. Chem. Soc.* **1987**, *108*, 846−856.
(31) Liddell, P. A.; Barrett, D.; Makings, L. R.; Pessiki, P. J.; Gust, D.; Moore, T. A. *J. Am. Chem. Soc.* **1986**, *108*, 5350−5352.
(32) Gust, D. *Nature* **1997**, *386* (6620), 21−22.
(33) Harriman, A.; Hissler, M.; Trompette, O.; Ziessel, R. *J. Am. Chem. Soc.* **1999**, *121* (11), 2516−2525.
(34) Coe, B. J.; Friesen, D. A.; Thompson, D. W.; Meyer, T. J. *Inorg. Chem.* **1996**, *35* (16), 4575−4584.
(35) Borowicz, P.; Herbich, J.; Kapturkiewicz, A.; Opallo, M.; Nowacki, J. *Chem. Phys.* **1999**, *249* (1), 49−62.
(36) Chen, Y.-D.; Qin, Y.-H.; Zhang, L.-Y.; Shi, L.-X.; Chen, Z.-N. *Inorg. Chem.* **2004**, *43*, 1197−1205.
(37) Connick, W. B.; Miskowski, V. M.; Houlding, V. H.; Gray, H. B. *Inorg. Chem.* **2000**, *39* (12), 2585−2592.
(38) Hissler, M.; McGarrah, J. E.; Connick, W. B.; Geiger, D. K.; Cummings, S. D.; Eisenberg, R. *Coord. Chem. Rev.* **2000**, *208*, 115−137.
(39) Huertas, S.; Hissler, M.; McGarrah, J. E.; Lachicotte, R. J.; Eisenberg, R. *Inorg. Chem.* **2001**, *40* (6), 1183−1188.
(40) McGarrah, J. E.; Kim, Y.-J.; Hissler, M.; Eisenberg, R. *Inorg. Chem.* **2001**, *40*, 4510−4511.
(41) Zuleta, J. A.; Bevilacqua, J. M.; Eisenberg, R. *Coord. Chem. Rev.* **1992**, *111*, 237−248.
(42) Zuleta, J. A.; Bevilacqua, J. M.; Proserpio, D. M.; Harvey, P. D.; Eisenberg, R. *Inorg. Chem.* **1992**, *31*, 2396−2404.
(43) Zuleta, J. A.; Bevilacqua, J. M.; Rehm, J. M.; Eisenberg, R. *Inorg. Chem.* **1992**, *31*, 1332−1337.
(44) Zuleta, J. A.; Bevilacqua, J. M.; Eisenberg, R. *Coord. Chem. Rev.* **1991**, *111*, 237−248.
(45) Zuleta, J. A.; Burberry, M. S.; Eisenberg, R. *Coord. Chem. Rev.* **1990**, *97*, 47−64.
(46) Zuleta, J. A.; Chesta, C. A.; Eisenberg, R. *J. Am. Chem. Soc.* **1989**, *111*, 8916−8917.
(47) Bevilacqua, J. M.; Zuleta, J. A.; Eisenberg, R. *Inorg. Chem.* **1994**, *33*, 258−266.
(48) Bevilacqua, J. M.; Eisenberg, R. *Inorg. Chem.* **1994**, *33*, 2913−2923.
(49) Bevilacqua, J. M.; Eisenberg, R. *Inorg. Chem.* **1994**, *33*, 1886−1890.
(50) Cummings, S. D.; Eisenberg, R. *Inorg. Chem.* **1995**, *34*, 3396−3404.
(51) Cummings, S. D.; Eisenberg, R. *Inorg. Chem.* **1995**, *34*, 2007−2014.
(52) Cummings, S. D.; Eisenberg, R. *J. Am. Chem. Soc.* **1996**, *118*, 1949−1960.
(53) Cummings, S. D.; Eisenberg, R. *Inorg. Chim. Acta* **1996**, *242*, 225−231.
(54) Paw, W.; Cummings, S. D.; Mansour, M. A.; Connick, W. B.; Geiger, D. K.; Eisenberg, R. *Coord. Chem. Rev.* **1998**, *171*, 125−150.
(55) Hissler, M.; Connick, W. B.; Geiger, D. K.; McGarrah, J. E.; Lipa, D.; Lachicotte, R. J.; Eisenberg, R. *Inorg. Chem.* **2000**, *39*, 447−457.
(56) Wadas, T. J.; Lachicotte, R. J.; Eisenberg, R. *Inorg. Chem.* **2003**, *42* (12), 3772−3778.
(57) Cummings, S. D.; Eisenberg, R. *Prog. Inorg. Chem.* **2003**, *52*, 315−367.
(58) Chan, C.-W.; Cheng, L.-K.; Che, C.-M. *Coord. Chem. Rev.* **1994**, *132*, 87−97.
(59) Whittle, C. E.; Weinstein, J. A.; Geore, M. W.; Schanze, K. S. *Inorg. Chem.* **2001**, *40*, 4053−4062.
(60) Pomestchenko, I. E.; Luman, C. R.; Hissler, M.; Ziessel, R.; Castellano, F. N. *Inorg. Chem.* **2003**, *42* (5), 1394−1396.
(61) McGarrah, J. E.; Eisenberg, R. *Inorg. Chem.* **2003**, *42* (14), 4355−4365.
(62) Pangborn, A. B.; Giardello, M. A.; Grubbs, R. H.; Rosen, R. K.; Timmers, F. J. *Organometallics* **1996**, *15*, 1518−1520.
(63) Halbes, U.; Pale, P. *Tetrahedron Lett.* **2002**, *43*, 2039−2042.
(64) Kukushkin, V. Y.; Pombeiro, A. J. L. *Inorg. Synth.* **2002**, *33*, 189−195.
(65) Fanizzi, F. P.; Natile, G.; Lanfranchi, M.; Tiripicchio, A.; Laschi, F.; Zanello, P. *Inorg. Chem.* **1996**, *35* (11), 3173−3182.
(66) Kukushkin, V. Y.; Pombeiro, A. J. L.; Ferreira, C. M. P.; Elding, L. I.; Puddephatt, R. J. *Inorg. Synth.* **2002**, *33*, 189−196.
(67) Austin, W. B.; Bilow, N.; Kelleghan, W. J.; Lau, K. S. Y. *J. Org. Chem.* **1981**, *46* (11), 2280−2286.
(68) Sonogashira, K.; Takahashi, S.; Hagihara, N. *Macromol. Chem.* **1997**, 10, 879.

electrochemical analysis, it was estimated that the CS state of the triad (PTZ^{+}•-C−NO_2^{-}•) transiently stored ca. 1.7 V of energy.

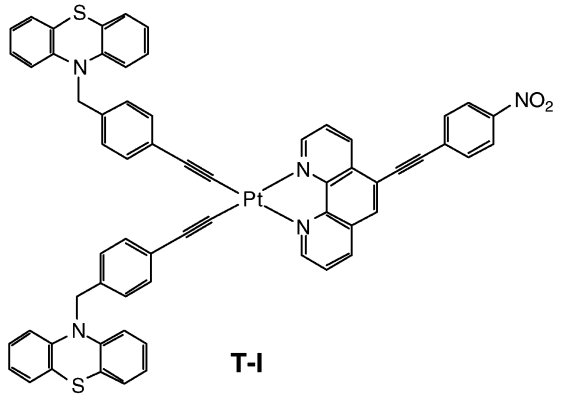

T-I

In the second study,[40,61] D−C dyads were prepared and studied in which 4,4′-diethoxycarbonylbipyridine and 4,4′-di-*tert*-butylbipyridine were the diimine ligands and phenothiazine and 2-trifluoromethylphenothiazine functioned as the one-electron donors. When the diimine was 4,4′-di-*tert*-butylbipyridine, emission intensity was observed to be solvent-dependent, with significant luminescence quenching occurring in polar solvents but not in nonpolar solvents. Intramolecular electron transfer was observed by transient absorption spectroscopy, and analysis of the photophysical and electrochemical data suggested that, whereas charge separation appeared to be in the Marcus normal region, charge recombination was found to be in the inverted region.

Although these Pt(II) diimine dyads and triads provided meaningful data and insight for photoinduced charge separation, their syntheses were arduous, utilizing a sequence of Pd^{2+}-catalyzed Sonogashira−Hagihara coupling steps, each with problems of purification and catalyst metal ion removal. As an alternative approach, we describe in this paper the synthesis and study of dyad systems constructed using Schiff base condensations to an aldehyde-containing Pt(diimine)-bis(arylacetylide) chromophore. We have previously described related Pt(diimine)(C≡C−*p*-$C_6H_4CHO)_2$ complexes that were brightly emissive in fluid solution with a ^{3}MLCT state characteristic of other arylacetylide derivatives,[56] and this study builds on that work. Representative D−C dyads were synthesized and structurally characterized, and their luminescence properties and relative stabilities upon irradiation are described.

Experimental Section

Reagents. Potassium tetrachloroplatinate (Johnson Matthey); 4,7-diphenylphenanthroline (dpphen), 4-trimethylsilylethynylbenzaldehyde, copper(I) iodide, aniline (ani), *N*,*N*′-(dimethylamino)-1,4-phenylenediamine (NMe_2ani) dihydrochloride, *p*-anisidine (MeOani), *N*-benzylidene aniline (**L-4**), *N*-benzylidene-*p*-anisidine (**L-3**), *N*,*N*′-dimethylformamide, absolute methanol, absolute ethanol, chloroform, triethylamine, zinc(II) chloride, glacial acetic acid (HOAc), and sodium triacetoxyborohydride (all from Aldrich); 1,4-benzene diamine (**L-2**) (ChemBridge Corporation); and tetrabutylammonium hexafluorophosphate (Fluka) were used without further purification. All solvents were of spectroscopic grade or better, triethylamine was distilled under nitrogen from potassium hydroxide, and methylene chloride, toluene, and acetonitrile were purified by passing the degassed solvent through columns of activated alumina and molecular sieves under argon as described in the literature.[62] The compounds $Pt(DMSO)_2Cl_2$, Pt(dpphen)-Cl_2,and 4-ethynylbenzaldehyde were prepared according to literature methods.[63−67] The syntheses of Pt(dpphen)$(arylacetylide)_2$ complexes and all dyads were performed under nitrogen or argon with degassed solvents following a procedure similar to that previously reported.[55,68−70]

Physical Measurements. ^{1}H NMR spectra were recorded on a Bruker AMX-400 or Avance 400 spectrometer (400 MHz), and infrared spectra were obtained from Nujol mulls, dry film, or KBr pellets using a Mattson Galaxy 6020 FTIR spectrometer. Field desorption mass spectrometry was performed by Kodak Analytical Services, Rochester, NY, and elemental analyses were provided by Desert Analytics, Tucson, AZ. Cyclic voltammetry experiments were conducted on a EG & G PAR 263 A potentiostat/galvanostat using a three-electrode single-cell compartment, and all samples were degassed with argon. A Pt wire working electrode, a Pt wire auxiliary electrode, and $Ag/AgNO_3$/acetonitrile reference electrode were used, and the scan rate used was 50 mV/s. For all measurements, tetrabutylammonium hexafluorophosphate was used as the supporting electrolyte with ferrocene as an internal reference, and all redox potentials are reported relative to the ferrocenium/ferrocene (Fc^{+}/Fc) couple (0.4 V versus SCE). Absorption spectra were recorded using a Hitachi U2000 scanning spectrophotometer (200−1100 nm). Steady-state luminescence spectra were measured on a Spex Fluoromax-P fluorometer and corrected for instrument response. Lifetime data of the chromophore were obtained using an excimer-pumped dye laser system (1−3 mJ/pulse) with the excited-state decay fit to single exponentials. The metal complex concentration was 3×10^{-5} M, and each sample was subjected to at least four freeze−pump−thaw cycles. Photolysis experiments were conducted in wet and anhydrous methylene chloride using a 1-cm quartz cuvette equipped with a high-vacuum valve and an Oriel Hg/Xe lamp with a filter to absorb all wavelengths below 300 nm. For studies examining dyad stabilities, absorption and emission spectra were recorded before and immediately after 1 h of irradiation and at arbitrary time points over the course of 3 days. Samples were kept in the absence of light until measurements were taken.

TMS−C≡C−C_6H_4−*p*-(CH=N−$C_6H_4NMe_2$) (L-2−CC−TMS). A 100-mL round-bottom flask was charged with 4-trimethylsilylethynylbenzaldehyde (1 g, 4 mmol), NMe_2ani (1.18 g, 5.6 mmol), and $ZnCl_2$ (10 mg). Twenty-five milliliters of CH_2Cl_2 containing 0.8 mL of Et_3N was added, and the resulting solution was allowed to stir at room temperature for 12 h. The solvent was removed, and the resultant solids were chromatographed on a Biotage 40S column (alumina, 40 μm, 60 Å) eluting with a solvent mixture of hexanes/CH_2Cl_2 (1:2 v/v) to give an orange solid. Yield: 79 mg (50%). ^{1}H NMR (CD_2Cl_2): δ 8.49 (1H, s), 7.61 (2H, d, J = 12 Hz), 7.52 (2 H, d, J = 8.0 Hz), 7.25 (2H, s), 6.76 (2H, s), 2.98 (6H, s), 0.25 (9H, s). MS (EI) *m*/*z* (%): 320 (100).

H−C≡C−C_6H_4−*p*-(CH_2−NH−$C_6H_4NMe_2$) (L-2a−CC−H). A 100-mL round-bottom flask was charged with **L-2−CC−TMS** (0.05 g, 0.156 mmol), $NaBH_4$ (0.06 g, 1.56 mmol), and 50 mL of dry methanol. The resultant solution was allowed to stir at room

(69) Sonogashira, K.; Yatake, T.; Tohda, Y.; Takahashi, S.; Hagihara, N. *J. Chem. Soc., Chem. Commun.* **1977**, 291.
(70) Sonogashira, K.; Fujikura, Y.; Yatake, T.; Toyoshima, N.; Takahashi, S.; Hagihara, N. *J. Org. Chem.* **1978**, *145*, 101−108.

temperature for 24 h, after which solvent was removed and the residue was dissolved in CH_2Cl_2 and filtered through a 2-in. pad of alumina. The resultant solution was dried to give a yellow solid. Yield: 39 mg (50%). ^{1}H NMR $CDCl_3$: δ 7.47 (2H, d, J = 8.12 Hz), 7.35 (2H, d, J = 8.04 Hz), 6.74 (2H, d, J = 8.88 Hz), 6.62 (2H, d, J = 8.8 Hz), 4.32 (2H, s), 3.07 (1H, s), 2.84 (6H, s), 1.56 (1H, s). MS (EI) *m*/*z* (%): 250 (100).

Pt(dpphen)(C≡CC$_6$H$_4$CHO)$_2$ (1). A Schlenk tube was charged with Pt(dpphen)Cl_2 (0.100 g, 0.17 mmol), 4-ethynylbenzaldehyde (0.21 g, 1.6 mmol), CuI (10 mg), and 10 mL of a solvent mixture of DMF/NEt_3 (8:2 v/v). The resultant heterogeneous solution was allowed to stir for 24 h at 65 °C, after which it was filtered through a medium-porosity glass frit. The precipitate was washed with methanol, ethanol, and diethyl ether, recrystallized from CH_2Cl_2, washed with methanol and diethyl ether, and dried under vacuum. X-ray-quality crystals were grown by the vapor diffusion of diethyl ether into saturated solutions of **1** in CH_2Cl_2 at room temperature. Yield: 109 mg (83%). ^{1}H NMR (CD_2Cl_2): δ 9.96 (2H, s), 9.92 (2H, d, J = 5.2 Hz), 8.09 (2H, s), 7.92 (2H, d, J = 4.80 Hz), 7.82 (4H, d, J = 8.4 Hz), 7.66 (4H, d, J = 8.0 Hz), 7.63 (10H, M). FT IR (dry film, cm^{-1}): 1689 (υ_{CHO}), 2125, 2113 ($\upsilon_{C\equiv C}$). MS (FD) *m*/*z* (%): 786.0 ([M]$^+$, 100). Anal. Calcd for $PtC_{42}H_{26}N_2O_2\cdot CH_3OH$: C, 64.20; H, 3.33; N, 3.56. Found: C, 63.71; H, 3.51; N, 3.45.

Pt(dpphen)[C≡CC$_6$H$_4$—*p*-(CH=N—C$_6$H$_4$NMe$_2$)]$_2$ (2). A 50-mL round-bottom flask was charged with **1** (0.05 g, 0.63 mmol), $ZnCl_2$ (10 mg), NMe_2ani·2HCl (0.0531 g, 2.5 mmol), and 20 mL of CH_2Cl_2/MeOH (4:1 v/v) containing NEt_3 (0.25 g, 2.5 mmol), and the resultant solution was allowed to stir for 40 h at room temperature. The product was isolated on a medium-porosity glass frit; washed with small amounts of methanol, ethanol, and diethyl ether; recrystallized from a methanol/CH_2Cl_2 mixture; washed with methanol and diethyl ether; and dried under vacuum. X-ray-quality crystals were grown by diffusion of ethanol into a saturated solution of **2** in CH_2Cl_2 at room temperature. Yield: 117 mg (90%). ^{1}H NMR (CD_2Cl_2): δ 9.95 (2H, d, J = 4 Hz), 8.50 (2H, s), 8.08 (2H, s), 7.90 (2H, d, J = 4 Hz), 7.83 (4H, d, J = 8 Hz), 7.64 (14H, m), 7.28 (4H, d, J = 8 Hz), 6.77 (4H, d, J = 8 Hz), 2.90 (12H, s). FT IR (dry film, cm^{-1}): 1617, 1600 ($\upsilon_{C=N}$), 2120 (sh), 2100 ($\upsilon_{C\equiv C}$). MS (FD) *m*/*z* (%): 1021.2 ([M]$^+$, 100). Anal. Calcd for $PtC_{58}H_{46}N_6\cdot 2CH_3OH$: C, 66.34; H, 5.01; N, 7.73. Found: C, 66.22; H, 4.38; N, 7.89.

Pt(dpphen)[C≡CC$_6$H$_4$—*p*-(CH=N—C$_6$H$_4$OMe)]$_2$ (3). A 50-mL round-bottom flask was charged with **1** (0.05 g, 0.63 mmol), $ZnCl_2$ (10 mg), MeOani (0.0531 g, 2.5 mmol), and 20 mL of CH_2Cl_2 containing 2 drops of HOAc, and the resultant solution was allowed to stir for 40 h at room temperature. The product was isolated on a medium-porosity glass frit; washed with small amounts of methanol, ethanol, and diethyl ether; recrystallized from a methanol/CH_2Cl_2 mixture; washed with methanol and diethyl ether; and dried under vacuum. X-ray-quality crystals were grown by the liquid diffusion of ethanol into a saturated solution of **3** in CH_2Cl_2 at room temperature. Yield: 114 mg (90%). ^{1}H NMR (CD_2Cl_2): δ 9.98 (2H, d, J = 4 Hz), 8.48 (2H, s), 8.09 (2H, s), 7.92 (2H, d, J = 8 Hz), 7.84 (4H, d, J = 8 Hz), 7.64 (14H, m), 7.25 (4H, d, J = 8 Hz), 6.95 (4H, d, J = 12 Hz), 3.82 (6H, s). MS (FD) *m*/*z* (%): 996.2 ([M]$^+$, 100). FT IR (dry film, cm^{-1}): 1620, 1600 ($\upsilon_{C=N}$), 2100 ($\upsilon_{C\equiv C}$). Anal. Calcd for $PtC_{56}H_{40}N_4O_2\cdot CH_3OH$: C, 66.59; H, 4.31; N, 5.44. Found: C, 66.80; H, 4.25; N, 5.42.

Pt(dpphen)[C≡CC$_6$H$_4$—*p*-(CH=N—C$_6$H$_5$)]$_2$ (4). A 25-mL round-bottom flask was charged with **1** (0.050 g, 0.63 mmol), $ZnCl_2$ (10 mg), 3 mL of aniline, and 20 mL of $CHCl_3$. The resulting solution was allowed to stir for 36 h at 60 °C. After being allowed to cool, the solution was filtered and concentrated, and ethanol was added. The solids were collected on a medium-porosity glass frit, washed with diethyl ether, recrystallized from a methanol/CH_2Cl_2 mixture, washed with methanol and diethyl ether, and dried under vacuum. X-ray-quality crystals were grown by the vapor diffusion of diethyl ether into a saturated solution of **4** in $CHCl_3$ at room temperature. Yield: 107 mg (90%). ^{1}H NMR (CD_2Cl_2): δ 10.01 (2H, d, J = 8 Hz), 8.46 (2H, s), 8.09 (2H, s), 7.93 (4H, d, J = 4 Hz), 7.86 (2H, d, J = 8 Hz), 7.67 (14H, pseudo t, J = 8 Hz), 7.43 (4H, pseudo t, J = 8 Hz), 7.27 (4H, d, J = 8 Hz). FT IR (dry film, cm^{-1}): 1608 ($\upsilon_{C=N}$), 2106 ($\upsilon_{C\equiv C}$). MS (FD) *m*/*z* (%) 936.0 ([M]$^+$, 100). Anal. Calcd for $PtC_{54}H_{36}N_4\cdot CHCl_3$: C, 62.59; H, 3.53; N, 5.30. Found: C, 63.02; H, 3.81; N, 5.55.

Pt(dpphen)[C≡CC$_6$H$_4$—*p*-(CH$_2$—NH—C$_6$H$_4$NMe$_2$)]$_2$ (2a). A 50-mL round-bottom flask was charged with **2** (0.05 g, 0.63 mmol), sodium triacetoxyborohydride (0.676 g, 3.1 mmol), and 50 mL of dichloromethane. The resultant solution was stirred for 48 h. The solution was then poured over water and extracted with dichloromethane (5 × 50 mL), dried with $MgSO_4$, filtered, and evaporated to dryness to give the desired product. The crude material was recrystallized from a CH_2Cl_2/C_2H_5OH (1:1 v/v) solution. Yield: 60 mg (60%). ^{1}H NMR (CD_2Cl_2): δ 10.00 (2H, d, J = 5.32 Hz), 8.06 (2H, s), 7.87 (2H, d, J = 5.4 Hz), 7.61 (10H, m), 7.49 (4H, d, J = 8.08 Hz), 7.31 (4H, d, J = 8.2 Hz), 6.70 (4H, d, J = 8.72 Hz), 6.62 (4H, d, J = 8.72 Hz), 4.28 (4H, s), 2.78 (12H, s), 1.5 (2H, s). FT IR (dry film, cm^{-1}): 2109 ($\upsilon_{C\equiv C}$), 2963 (υ_{C-H}), 3390 (υ_{N-H}). MS (FD) *m*/*z* (%): 1024.4 ([M]$^+$, 100). Anal. Calcd for $PtC_{58}H_{50}N_6\cdot 2CH_2Cl_2\cdot 3.5C_2H_5OH$: C, 59.28; H, 5.58; N, 6.19. Found: C, 59.82; H, 5.52; N, 5.71.

Pt(dpphen)[C≡CC$_6$H$_4$—*p*-(CH$_2$—NH—C$_6$H$_4$OMe)]$_2$ (3a). The same procedure as employed for **2a** was followed except that complex **3** (0.05 g, 0.63 mmol) was used as the starting material. Yield: 55 mg (55%). ^{1}H NMR (CD_2Cl_2): δ 10.13 (2H, d, J = 5.4 Hz), 8.16 (2H, s), 7.99 (2H, d, J = 5.4 Hz), 7.73 (10H, m), 7.62 (4H, d, J = 8.08 Hz), 7.42 (4H, d, J = 7.41 Hz), 6.85 (4H, d, J = 8.96 Hz), 6.72 (4H, d, J = 8.96 Hz), 4.39 (4H, s), 3.81 (6H, s), 1.63 (2H, s). FT IR (dry film, cm^{-1}): 1244 (υ_{OCH3}), 2112 ($\upsilon_{C\equiv C}$), 2928 (υ_{C-H}), 3390 (υ_{N-H}). MS (FD) *m*/*z* (%): 1000 ([M]$^+$, 100). Anal. Calcd for $PtC_{56}H_{44}N_4O_2\cdot CH_2Cl_2\cdot 3C_2H_5OH\cdot 0.5H_2O$: C, 61.40; H, 5.33; N, 4.54. Found: C, 61.65; H, 5.32; N, 3.92.

Pt(dpphen)(C≡CC$_6$H$_4$CH$_2$—*p*-NH—C$_6$H$_5$)$_2$ (4a). The same procedure as employed for **2a** was followed except that complex **4** (0.05 g, 0.63 mmol) was used as the starting material. X-ray-quality crystals were grown by the slow liquid diffusion of ethanol into a saturated solution of **4a** in dichloromethane at room temperature. Yield: 70 mg (70%). ^{1}H NMR (CD_2Cl_2): δ 10.05 (2H, d, J = 5.32 Hz), 8.09 (2H, s), 7.91 (2H, d, J = 5.44 Hz), 7.64 (10H, m), 7.54 (4H, d, J = 8.08 Hz), 7.34 (4H, d, J = 8.08 Hz), 7.18 (4H, t, J = 8, 7.96 Hz), 6.70 (6H, m), 4.36 (4H, s), 1.55 (2H, s). FT IR (dry film, cm^{-1}): 2112 ($\upsilon_{C\equiv C}$), 2928 (υ_{C-H}), 3390 (υ_{N-H}). MS (FD) *m*/*z* (%): 938.29 ([M]$^+$, 100). Anal. Calcd for $PtC_{54}H_{40}N_4$: C, 69.00; H, 4.29; N, 5.96. Found: C, 68.53; H, 4.11; N, 5.76.

X-ray Structural Determinations of 1−4 and 4a. Crystals of each complex were mounted under paratone-8277 oil on a glass fiber and immediately placed in a cold nitrogen stream at −80 °C on the X-ray diffractometer. It should be noted that **3** undergoes rapid solvent loss. The X-ray intensity data were collected on a standard Siemens SMART CCD area detector system equipped with a normal-focus molybdenum-target X-ray tube operated at 2.0 kW (50 kV, 40 mA). Data (1.3 hemispheres) were collected using a narrow-frame method with scan widths of 0.3° in ω and exposure times of 30 s/frame using a detector-to-crystal distance of 5.09 cm

Table 1. Crystallographic Data for Complexes **1**−**4** and **4a**·Et_2O

	1	**2**	**3**	**4**	**4a**·Et_2O
emp formula	$C_{42}H_{26}N_2O_2Pt$	$C_{58}H_{46}N_6Pt$	$C_{56}H_{40}N_4O_2Pt$	$C_{54}H_{36}N_4Pt$	$C_{58}H_{50}N_4OPt$
fw	785.74	1022.10	996.01	935.96	1014.11
T, K	293	293	293	193	193
μ, Å	0.71073	0.71073	0.71073	0.71073	0.71073
cryst syst	triclinic	monoclinic	monoclinic	monoclinic	triclinic
space group	$P\bar{1}$	$C2/c$	$P2(1)/c$	$C2/c$	$P\bar{1}$
Z	2	4	4	4	2
a, Å[a]	9.4406(4)	30.1689(18)	19.4441(10)	22.954(6)	10.5336(13)
b, Å[a]	11.6495(5)	15.5466(8)	16.3369(9)	19.501(5)	11.6625(15)
c, Å[a]	14.6801(7)	9.7179(5)	15.2547(8)	11.044(3)	19.425(2)
α, deg[a]	101.0600(10)	90.00	90.00	90.00	98.245(2)
β, deg[a]	95.9300(10)	91.365(2)	108.6090(10)	118.036(3)	90.598(2)
γ, deg[a]	95.4580(10)	90.00	90.00	90.00	105.602(2)
V, Å^3	1565.06(12)	4556.6(4)	4592.4(4)	4363.5(19)	2271.6(5)
ρ_{calcd}, g cm^{-3}	1.667	1.490	1.441	1.425	1.483
μ, mm^{-1}	4.524	3.126	3.102	3.256	3.135
abs correction	SADABS[b]	SADABS[b]	SADABS[b]	SADABS[b]	SADABS[b]
transm range	0.570−0.928	0.737−0.928	0.787−0.928	[c]	0.468−1.000
θ range, deg	1.79−28.27	2.41−28.29	1.67−28.27	2.01−28.28	1.83−28.32
no. data	7117	5381	10551	5270	10529
no. params	424	296	570	267	577
GOF[d]	1.064	1.089	1.054	0.944	1.052
R1, wR2 [$I > 2\sigma(I)$][e]	0.0336, 0.0937	0.0208, 0.0546	0.0204, 0.0505	0.0515,[f] 0.1187[f]	0.0334, 0.0724
R1, wR2 (all data)[e]	0.0344, 0.0943	0.0229, 0.0554	0.0271, 0.0521	0.1256,[f] 0.1366[f]	0.0407, 0.0752

[a] It has been noted that the integration program SAINT produces cell constant errors that are unreasonably small because systematic error is not included. More reasonable errors might be estimated at 10 times the reported value. [b] The SADABS program is based on the method of Blessing; see Blessing, R. H. *Acta Crystallogr. A* **1995**, *51*, 33. [c] The transmission coefficient cannot be specified because the crystal dimensions were lost. [d] GOF = $\{\sum[w(F_o^2 - F_c^2)^2]/(n - p)\}^{1/2}$, where n and p denote the number of data points and the number of parameters, respectively. [e] R1 = $(\sum||F_o| - |F_c||)/\sum|F_o|$; wR2 = $\{\sum[w(F_o^2 - F_c^2)^2]/\sum[w(F_o^2)^2]\}^{1/2}$, where $w = 1/[\sigma^2(F_o^2) + (aP)^2 + bP]$ and $P = [\max(0,F_o^2) + 2F_c^2]/3$. [f] Solvent disorder within the crystal lattice and small crystal size contribute to higher R factors in this case, but the overall structural connectivity is confirmed and in agreement with the crystal structures of **2** and **3**.

(maximum 2θ angle of 56.5°). The total data collection time was approximately 13 h for each complex. Frames were integrated to a maximum 2θ angle with the Siemens SAINT program and corrected for absorption with the program SADABS. The structures were solved by direct methods and refined employing full-matrix least-squares on F^2. All non-H atoms of the metal complexes were refined with anisotropic thermal parameters, and the non-H atoms of the solvent (if present) were refined isotropically. The hydrogen atoms were included in idealized positions. Solvent molecules that did not refine regardless of disorder model were compensated using the SQUEEZE program. Final residuals along with unit cell, space group, data collection, and refinement parameters are presented in Table 1.

Results and Discussion

Synthesis and Characterization. Complex **1** was synthesized according to a previously reported route in which the chloride ligands were exchanged by the arylacetylide groups using a CuI-catalyzed procedure, as indicated in Scheme 1.[55,68−70] The synthesis of the imine-containing donor−chromophore dyads (**2-4**) was accomplished by standard Schiff base chemistry to afford the desired products in excellent yields. Synthesis of the amine dyads (**2a**−**4a**), which is shown in Scheme 2, also proceeds smoothly in the presence of the borohydride reducing agent. Tolerance of the Pt complexes for reagents such as borohydride and acetic acid demonstrates the robust nature of the former. The complexes are soluble in CH_2Cl_2 and DMF and only sparingly soluble in toluene. In addition, several benzaldimine compounds **L-4**, **L-3**, **L-2**, and **L-2**−**CC**−**TMS**, p-R−C_6H_5CH═N−p-C_6H_4−R′, (**L-4**, R = H, R′ = H; **L-3**, R = H, R′ = OMe; **L-2**, R = H, R′ = NMe_2; **L-2**−**CC**−**TMS**, R = TMS−C≡C$^-$, R′ = NMe_2) were purchased from respective suppliers or synthesized while amine **L-2a**−**CC**−**H** was prepared by the reaction of **L-2**−**CC**−**TMS** with borohydride (Scheme 3).

All of the complexes were characterized by NMR, IR, electronic absorption, and emission spectroscopies, mass spectroscopy, and elemental analyses. Additionally, complexes **1**−**4** and **4a** were structurally characterized by X-ray crystallography. All of the spectroscopic data are consistent with the X-ray structural results described below.

Molecular Structures of 1−4 and 4a. The molecular structures of the aldehyde-containing complex **1**, the imine dyad **2,** and the amine dyad **4a** are shown in Figures 1−3, respectively, with important bond lengths and angles for **1**, **2**, and **4a** reported in Table 2. Perspective drawings of the other imine dyads **3** and **4** and complete crystallographic information including all bond distances and angles for all structures are given in the Supporting Information. Each complex consists of a square-planar Pt(II) ion with a dpphen chelate and two cis acetylide ligands. The average Pt−N distance of 2.064(10) Å in the complexes agrees well with those of other Pt phenanthroline complexes such as 2.063(3), 2.033(6), and 2.040(5) Å in $Pt(phen)Cl_2$,[71] $Pt(phen)(C{\equiv}CC_6H_4CH_3)_2$,[55] and $Pt(dbbpy)(C{\equiv}CC_6H_4CH_3)_2$,[72] respectively. The Pt−C(acetylide) distances in all of the

(71) Hazell, A.; Mukhopadhyay, A. *Acta Crystallogr.* **1980**, *B36*, 1647−1649.

Scheme 1

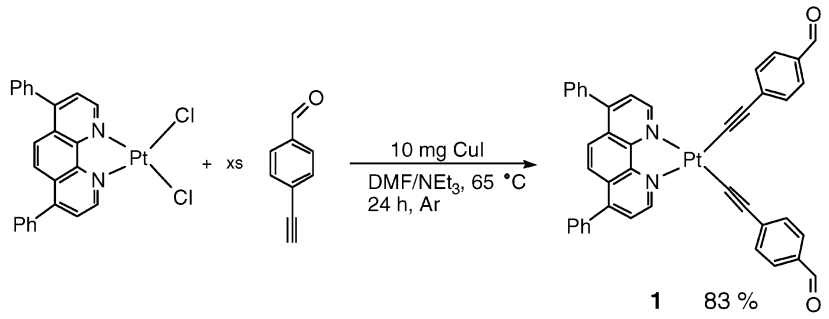

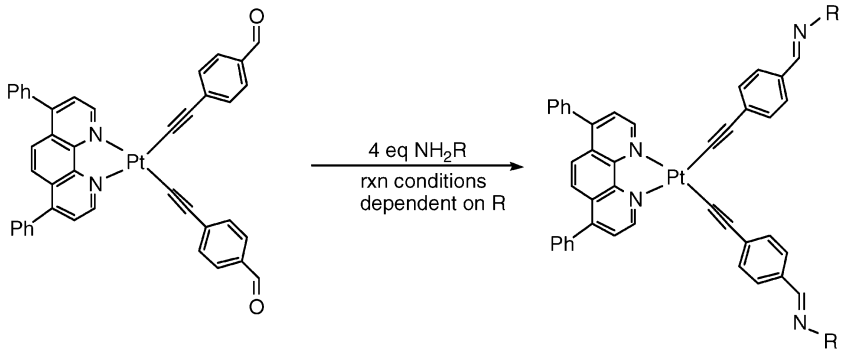

R	Reaction Conditions	Complex	Yield (%)
p-$C_6H_4NMe_2$	i	**2**	90
p-C_6H_4OMe	ii	**3**	90
p-C_6H_5	iii	**4**	90

i. $NH_2R = NH_2$-*p*-$C_6H_4NMe_2 \cdot 2HCl$, $ZnCl_2$, CH_2Cl_2/MeOH, NEt_3, 40 h, RT, Ar
ii. $ZnCl_2$, CH_2Cl_2, H^+, 40 h, RT, Ar
iii $ZnCl_2$, $CHCl_3$, 36 h, 60 C, Ar

Scheme 2

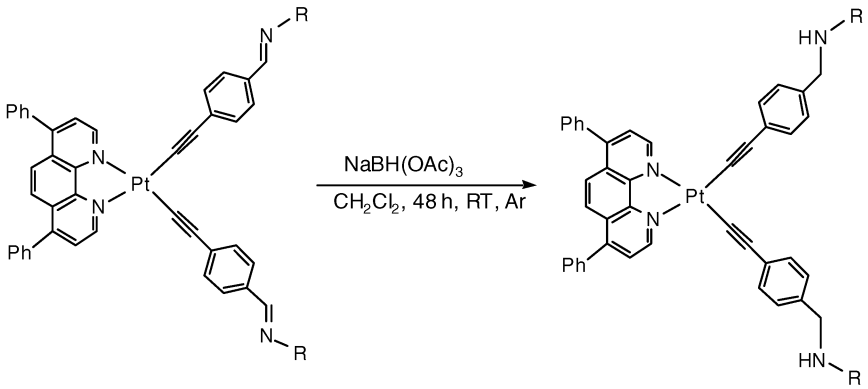

R	Complex	Yield (%)
p-$C_6H_4NMe_2$	**2a**	60
p-C_6H_4OMe	**3a**	55
p-C_6H_5	**4a**	70

structures reported here average 1.954(5) Å and this is in good agreement with previously reported Pt−C(acetylide) distances of 1.946(7) and 1.948(3) Å for Pt(phen)(C≡$CC_6H_4CHO)_2$[56] and Pt(phen)(C≡$CC_6H_4CH_3)_2$,[55] respectively. Deviations from a square-planar geometry for Pt(II) are relatively minor, with a mean C−Pt−C angle of 90.18(7)° and an average N−Pt−N bite angle of 79.27(9)°, the latter resulting from the built-in constraint of the chelated phenanthroline ligand. The average C=N (imine)[73−78] and C−N (amine)[79] bond distances, 1.255(3) and 1.423(5) Å, respec-

(72) James, S. L.; Younus, M.; Raithby, P. R.; Lewis, J. *J. Org. Chem.* **1997**, *543*, 233−235.

Scheme 3

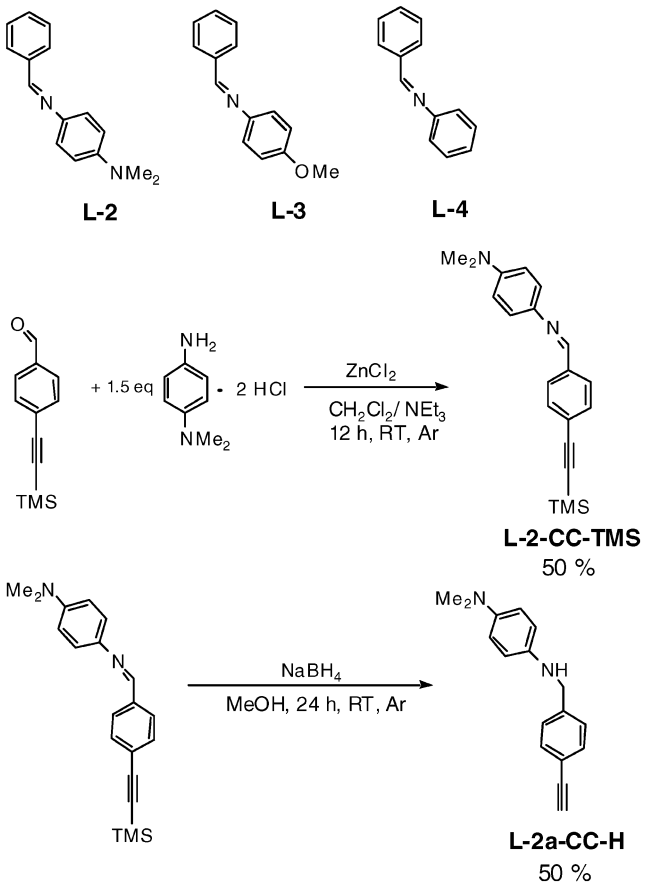

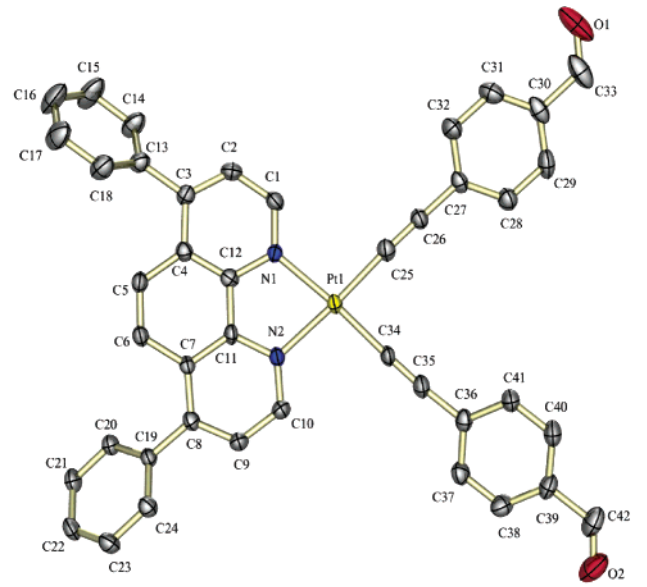

Figure 1. Crystal structure of **1** showing 80% probability ellipsoids. Hydrogen atoms and solvent molecules of crystallization have been omitted for clarity.

tively, agree well with previously reported examples. Finally, the phenyl rings located in the 4 and 7 positions of the phenanthroline ring are canted approximately 51° out of the phenanthroline plane most likely because of unfavorable steric interactions between the ortho protons located on those phenyl rings and the 5- and 6-position protons in the phenanthroline backbone.

Electrochemistry. All of the compounds were investigated by cyclic voltammetry, and the results are reported in Table

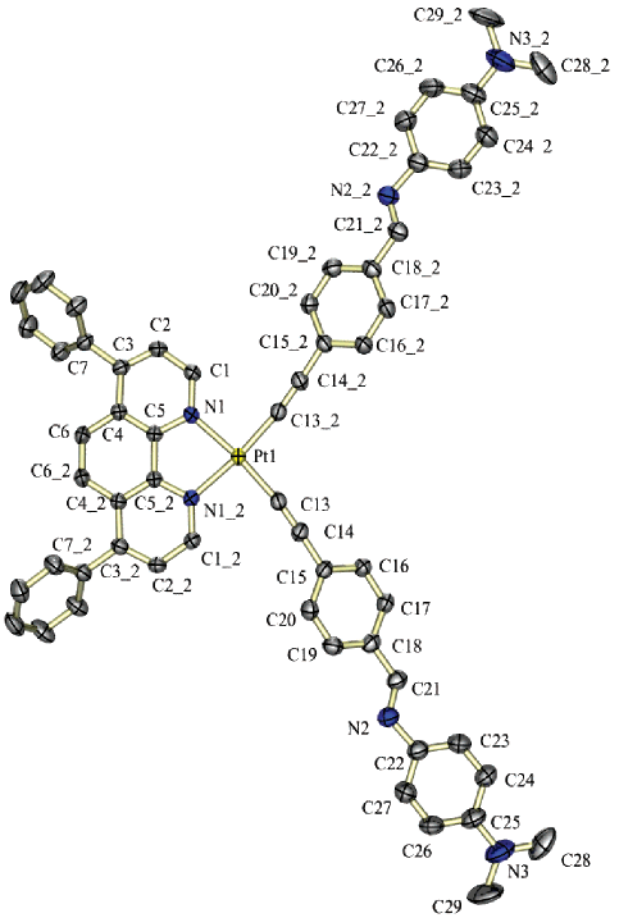

Figure 2. Crystal structure of **2** showing 80% probability ellipsoids. Hydrogen atoms and solvent molecules of crystallization have been omitted for clarity.

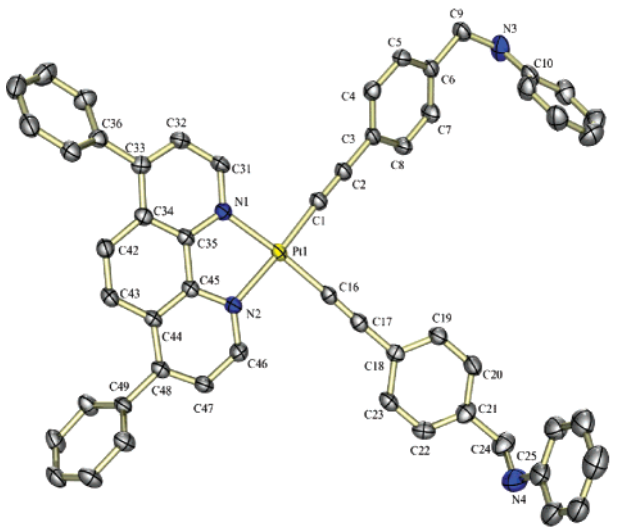

Figure 3. Crystal structure of **4a** showing 80% probability ellipsoids. Hydrogen atoms and solvent molecules of crystallization have been omitted for clarity.

(73) Koh, L. L.; Ranford, J.; Robinson, W.; Svensson, J. O.; Tan, A. L. C.; Wu, D. *Inorg. Chem.* **1996**, *35* (22), 6466−6472.
(74) Caravan, P.; Rettig, S. J.; Orvig, C. *Inorg. Chem.* **1997**, *36* (21), 4912.

Table 2. Selected Bond Lengths (Å) and Angles (deg) for Complexes **1**, **2**, and **4a**·Et_2O

bond lengths		bond angles	
		Complex **1**	
Pt(1)−C(25)	1.961(5)	C(34)−Pt(1)−C(25)	87.18(17)
Pt(1)−C(34)	1.959(4)	C(25)−Pt(1)−N(1)	97.10(16)
Pt(1)−N(1)	2.068(3)	C(34)−Pt(1)−N(2)	96.32(15)
Pt(1)−N(2)	2.068(3)	N(1)−Pt(1)−N(2)	79.40(13)
C(25)−C(26)	1.195(6)	C(25)−Pt(1)−N(2)	176.09(14)
C(34)−C(35)	1.192(6)	C(34)−Pt(1)−N(1)	175.72(13)
		Complex **2**	
Pt(1)−C(13)	1.951(2)	C(13)−Pt(1)−C(13) #1	92.93(13)
Pt(1)−N(1)	2.0618(18)	C(13) #1−Pt(1)−N(1)	93.83(8)
C(13)−C(14)	1.206(3)	N(1)−Pt(1)−N(1) #1	79.56(10)
		C(13)−Pt(1)−N(1)	172.75(8)
		Complex **4a**·Et_2O	
Pt(1)−C(1)	1.956(4)	C(16)−Pt(1)−C(1)	87.68(14)
Pt(1)−C(16)	1.939(3)	C(16)−Pt(1)−N(2)	95.58(12)
Pt(1)−N(1)	2.070(3)	C(1)−Pt(1)−N(1)	97.56(13)
Pt(1)−N(2)	2.062(3)	N(2)−Pt(1)−N(1)	79.42(11)
C(1)−C(2)	1.205(5)	C(1)−Pt(1)−N(2)	174.74(13)
C(16)−C(17)	1.209(5)	C(16)−Pt(1)−N(1)	173.91(12)

Table 3. Quantum Yields and Redox Potentials (V vs Fc^+/Fc)[a]

compound	ϕ_{em} (%)[b]	E (V)/ΔE (mV)
1	36	1.04,[c] −1.7 (100)
2	0.002	0.28,[d] −1.75 (100)
3	0.02	0.26,[d] 0.80,[d] −1.74 (80)
4	0.07	0.61,[d] −1.73 (90)
2a	0.0036	−0.24,[d] 0.36,[d] −1.76 (90)
3a	0.032	0.24,[d] −1.76 (110)
4a	0.4008	0.45,[d] −1.75 (110)
L-2		0.24,[d] 0.55[d]
L-3		0.87,[d] 1.51[d]
L-4		1.30[d]

[a] In 2:1 dichloromethane/acetonitrile solution at 50 mV/s containing 0.1 M tetrabutylammonium hexafluorophosphate at 298 K. [b] Determined using $Ru(bpy)_3^{2+}$ as the standard. [c] Irreversible and poorly defined under experimental conditions. [d] Irreversible under experimental conditions.

3 with all potentials given relative to the Fc^+/Fc couple used as an internal standard. The complexes show irreversible oxidation and quasireversible reduction processes. The electrochemical behavior of complex **1** is similar to that reported previously for similar systems.[55] Complex **1** shows one poorly defined irreversible oxidation wave at 1.04 V and one reversible reduction corresponding to the addition of an electron to an orbital of the diimine ligand at −1.7 V.

The amine and imine complexes undergo oxidation following the order of oxidation: **2** (NMe_2ani) more easily than **3** (MeOani) more easily than **4** (ani).[80,81] This trend is further confirmed from the respective imine ligands, which follow the same order, as oxidation of **L-2** is easier than that of

(75) Fernandez-G, J. M.; del Rio-Portilla, F.; Quiroz-Garcia, B.; Toscano, R. A.; Salcedo, R. *J. Mol. Struct.* **2001**, *561* (1−3), 197−207.
(76) Dahan, F.; Dyer, P. W.; Hanton, M. J.; Jones, M.; Mingos, D. M. P.; White, A. J. P.; Williams, D. J.; Williamson, A.-M. *Eur. J. Inorg. Chem.* **2002**, *3*, 732−742.
(77) Albietz, P. J., Jr.; Yang, K.; Eisenberg, R. *Organometallics* **1999**, *18* (15), 2747−2749.
(78) Albietz, P. J., Jr.; Yang, K.; Lachicotte, R. J.; Eisenberg, R. *Organometallics* **2000**, *19* (18), 3543−3555.
(79) Marcazzan, P.; Patrick, B. O.; James, B. R. *Organometallics* **2003**, *22*, 1177−1179.
(80) Meites, L.; Zuman, P.; Rupp, E. B. *CRC Handbook Series in Organic Electrochemistry*; CRC Press: Boca Raton, FL, 1982.
(81) Brookes, B. A.; Lawrence, N. S.; Compton, R. G. *J. Phys. Chem. B* **2000**, *104*, 11258−11267.

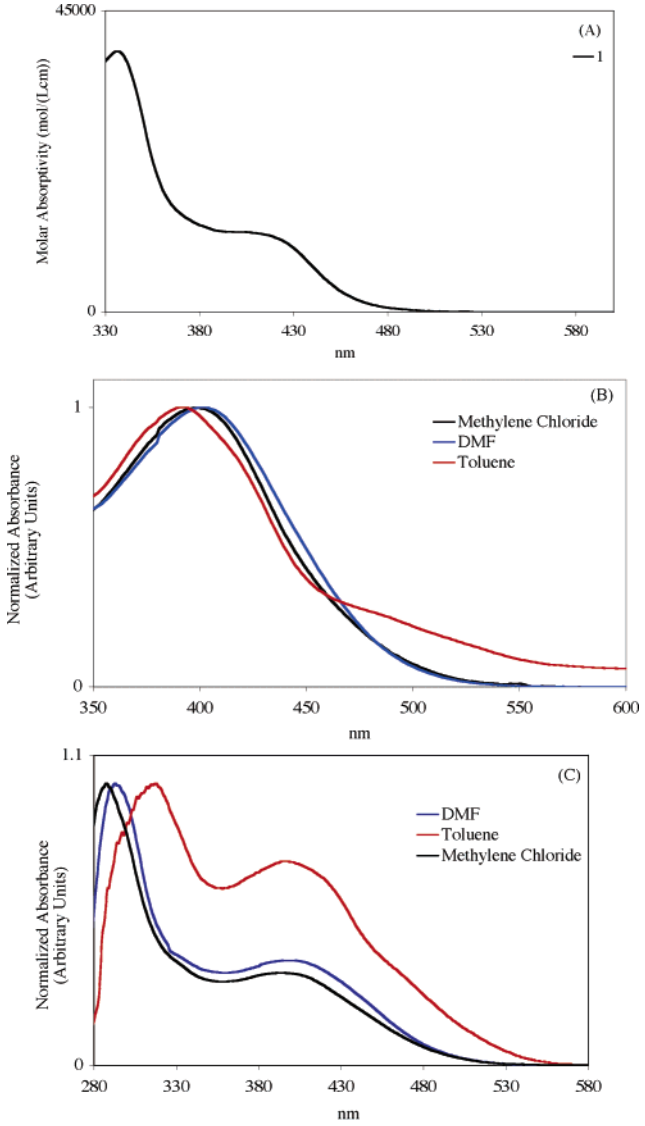

Figure 4. (A) Room-temperature absorption spectrum of **1** in CH_2Cl_2. (B) Normalized room-temperature absorption spectra of **2** in DMF, CH_2Cl_2, and toluene. (C) Normalized room-temperature absorption spectra of **2a** in DMF, CH_2Cl_2, and toluene.

L-3, which, in turn, is easier than that of **L-4**. With regard to the imine ligands as well as the imine complexes, the first oxidation is most probably donor-based, following a trend reflecting the relative ease of aryl oxidation as one moves from aniline to MeO- and NMe_2-anilines. There is also a second oxidation wave for the imine ligands **L-2** and **L-3** as well as the imine complex **3**. For the amine complexes, the lowest irreversible oxidation follows the same trend as that seen for the imine complexes, with oxidation of **2a** at a lower potential than that of **3a**, which is again lower (less anodic) than that of **4a**. The amine complex **2a** also shows a second oxidation wave. However, the basis of the second oxidation waves for both complexes **3** and **2a** and ligands **L-2** and **L-3** is not established at this point.

Absorption Spectra. The absorption spectra of all of the complexes have been measured in methylene chloride, DMF, and toluene (Figures 4, S4, and S5). The high-energy bands (λ < 370 nm) assignable as diimine-, imine-, amine-, and acetylide-based intraligand transitions are readily apparent.

Complexes **1**, **3**, **3a**, **4**, and **4a** exhibit an absorption around 400 nm that has been assigned as the Pt → π^*(diimine) ^{1}MLCT transition.[55,59] The transition comprising the 400-nm band progressively shifts to lower energy as the electron-donating ability of the arylacetylide ligand increases [**1** (400 nm) > **4** (425 nm) > **3** (434 nm)]. The MLCT absorption of complexes **1**, **3**, **3a**, **4**, and **4a** undergoes a shift in λ_{max} as solvent polarity is changed (Figures 4, S4, and S5). This shift to higher energy with increasing solvent polarity corresponds to negative solvatochromism, suggesting that the ground state is more polar than the respective excited states. Similar solvatochromism has been described for other Pt(diimine)bis(acetylide) complexes as well as for Pt(diimine)dithiolate systems.[44,45,55]

In the case of **2** and **2a**, an intense absorption around 400 nm ($\epsilon = 7 \times 10^4$ L/mol·cm) is seen. The intensity of this band is much larger than that of the MLCT transition of **1**, **3**, **3a**, **4**, and **4a** (ϵ = 8000−20000 L/mol·cm) and exhibits only a very minor dependence on solvent polarity (Figure S3). In view of these differences from the MLCT transitions in other Pt(diimine)bis(acetylide) complexes, the intense 400-nm band for **2** and **2a** is not assigned to be the same MLCT transition.

To further probe the nature of the intense 400-nm transition, the absorption spectra of **L-4**, **L-3**, **L-2**, and **L-2**−**CC**−**TMS** were recorded in methlyene chloride, and their normalized absorption spectra are presented in Figure 5. All three imine (**L-4**−**L-2**) analogues display the same transition, which becomes more intense and shifts to lower energy as the degree of electron donation increases [**L-4** (313 nm) > **L-3** (336 nm) > **L-2** (380 nm)]. Figure 5 also demonstrates that this transition continues to shift to lower energy [**L-2** (380 nm) > **L-2**−**CC**−**TMS** (403 nm)] when an electron-withdrawing acetylide group is positioned para to the imine bond. Finally, the normalized absorption spectra of **L-2**−**CC**−**TMS**, **L-2a**−**CC**−**H**, and complexes **2** and **2a** are compared in Figure 5. Both **L-2**−**CC**−**TMS** and **L-2a**−**CC**−**H** exhibit the same feature at approximately 400 nm, suggesting that this transition in **2** and **2a** is ligand-based and obscures the less strongly allowed MLCT transitions. Based on literature reports, the intense band at 400 nm occurs in highly conjugated systems and has been assigned as a low-lying $\pi-\pi^*$ transition.[82,83]

Emission Spectroscopy of 1. Complex **1**, like other Pt(diimine)bis(acetylide) complexes, is highly emissive in fluid solution and displays a broad structureless emission. The relative quantum yield for emission of **1** in CH_2Cl_2 was measured using $Ru(bpy)_3^{2+}$ as the standard ($\phi = 0.062$) and found to be 36%, which is similar to what has been reported for other complexes of this type.[84] Complex **1** has an excited state with a long lifetime of 3.1 μs that is approximately 10 times longer-lived, as well as 10 times more luminescent, than that of the corresponding phenanthroline complex, Pt(phen)(C≡C−*p*-$C_6H_4CHO)_2$.[56] The basis of the long excited-state lifetime can be found in a rationalization put forward by McCusker to explain the long excited-state lifetimes of related Ru(II) dpphen systems.[85,86] Specifically, in the excited state, the phenyl substituents on the dpphen ligand rotate into the plane of the phenathroline to create a more highly conjugated ligand, resulting in greater delocalization of the excited-state electron. Based on the measured values of τ and ϕ_{rel}^{em}, the radiative and nonradiative rate constants for **1** are calculated to be $k_r = 1.2 \times 10^5$ s^{-1} and $k_{nr} = 2.1 \times 10^5$ s^{-1}.

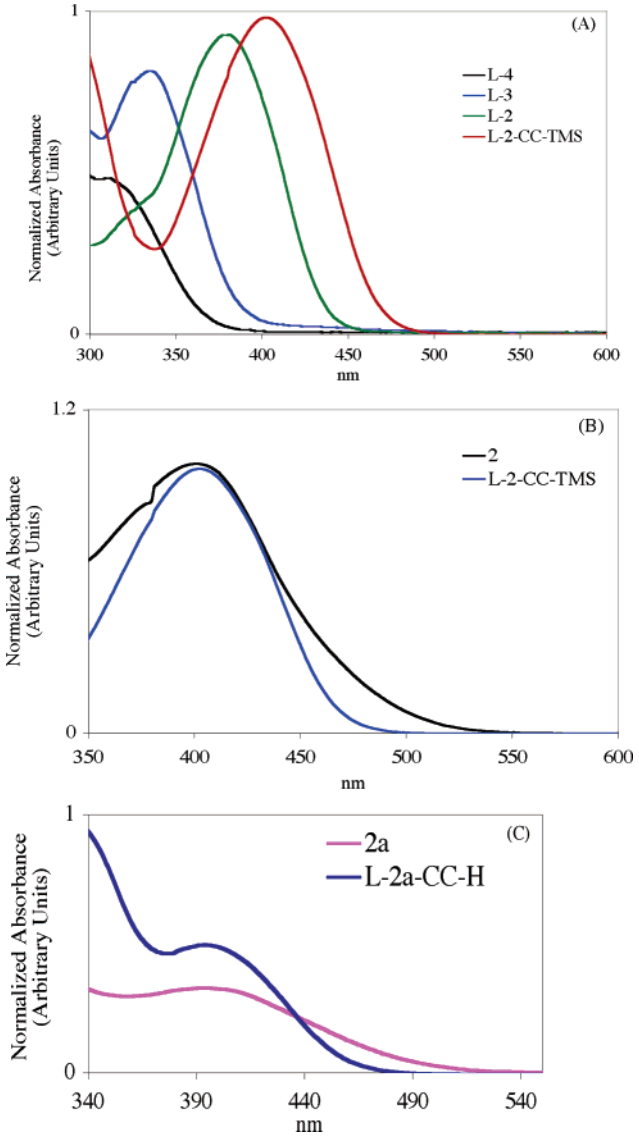

Figure 5. (A) Normalized room-temperature absorption spectra of **L-4**, **L-3**, **L-2**, and **L-2**−**CC**−**TMS** in CH_2Cl_2. (B) Normalized room-temperature absorption spectra of **2** and **L-2**−**CC**−**TMS** in CH_2Cl_2 at room temperature. (C) Normalized room-temperature absorption spectra of **2a** and **L-2a**−**CC**−**H** in CH_2Cl_2 at room temperature.

Emission of Dyads, Quenching, and Photodecomposition. Substantial luminescence quenching is observed for all of the D−C dyads when compared to **1**, and this can be seen

(82) Smith, W. F. *Tetrahedron* **1963**, *19*, 445−454.
(83) Reeves, R. L.; Smith, W. F. *J. Am. Chem. Soc.* **1963**, *85*, 724−728.
(84) Chan, S.-C.; Chan, M. C. W.; Wang, Y.; Che, C.-M.; Cheung, K.-K.; Zhu, N. *Chem. Eur. J.* **2001**, *7*, 4180−4190.
(85) Damrauer, N. H.; McCusker, J. K. *J. Phys. Chem. A* **1999**, *103* (42), 8440−8446.
(86) Damrauer, N. H.; Boussie, T. R.; Devenney, M.; McCusker, J. K. *J. Am. Chem. Soc.* **1997**, *119* (35), 8253−8268.

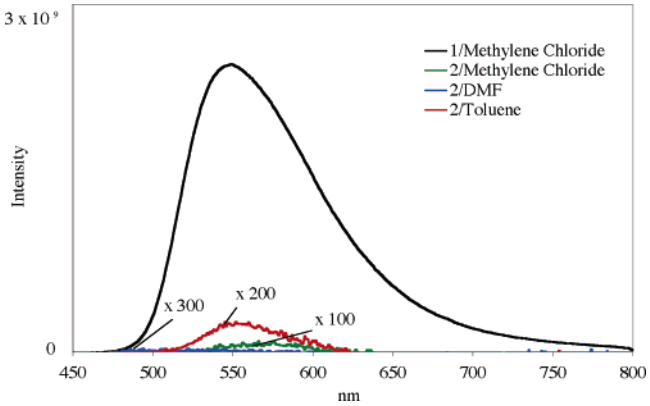

Figure 6. Emission spectrum of the chromophore in CH_2Cl_2 at room temperature and spectra of **2** in solvents of varying polarity. Multiplication factors are arbitrary so that the emission spectra can be observed for each solvent and compared relative to that of chromophore **1**.

from Figures 6 and S6, but unlike other dyads based on the Pt(diimine)bis(acetylide) chromophore,[61] luminescence quenching is not solvent-dependent. A tabulation of relative quantum yields obtained in degassed methylene chloride is presented in Table 3 and correlates well with the standard potentials of the donors aniline, MeO-aniline and NMe_2-aniline. Because NMe_2-aniline is the most easily oxidized of the three donors, reductive quenching of the ^{3}MLCT excited state would be the most efficient in this dyad, yielding a substantially lower relative quantum yield for emission. Conversely, aniline is the most difficult to oxidize, making reductive quenching of the excited state less facile with consequent increased luminescence. As expected, the imine dyads were observed to have lower relative quantum yields than their amine analogues, suggestive of greater quenching due to conjugation between the donor and metal center. However, even with the most luminescent D−C dyad, the relative emission quantum yield was observed to be less than 0.5%, clearly indicating that the Pt chromophore undergoes effective reductive quenching with photooxidation of the donor. As has been observed for other Pt(diimine) systems, the quenching occurs through an electron-transfer mechanism and not through energy transfer.[49,56,87] Attempts to observe the charge-separated state directly in these systems, however, proved unsuccessful, and in the course of these measurements, it was found that the dyads were unstable chemically upon irradiation.

To investigate the photoinstability of these dyads, photolysis experiments were conducted on all of the samples, and a representative set of these experiments (imine complex **2** and amine complex **2a)** is discussed below. When complex **2** is irradiated in dry methylene chloride, the 400-nm transition is seen to decrease only during irradiation (Figure S7A), but in the presence of water, the same band continues to decrease even after irradiation ceases, indicating that a thermal reaction is taking place in the absence of further irradiation (Figure S7B).

Prior to irradiation, complex **2** in *dry* methylene chloride is very weakly emissive, whereas after photolysis, luminescence increases slightly with a blue shift from 586 to 567 nm, suggesting that a new species slowly forms after photolysis (Figure 7A). When a similar photolysis of **2** in *wet* dichloromethane is conducted, bright luminescence returns to the solution with an emission maximum of 550 nm, identical to that of chromophore **1** (Figure 7B). The new species formed was identified by FTIR spectroscopy. The band at 1620 cm^{-1} corresponding to the imine C═N stretch for **2** diminishes upon photolysis in *wet* dichloromethane, and a new peak at 1683 cm^{-1}, corresponding to the aldehyde C═O stretch of chromophore **1**, appears. Thus, **2** is undergoing hydrolysis to regenerate a small concentration of the brightly emissive chromophore. However, attempts to identify the weakly emissive species formed upon irradiation of *dry* CH_2Cl_2 samples of **2** have not met with success.

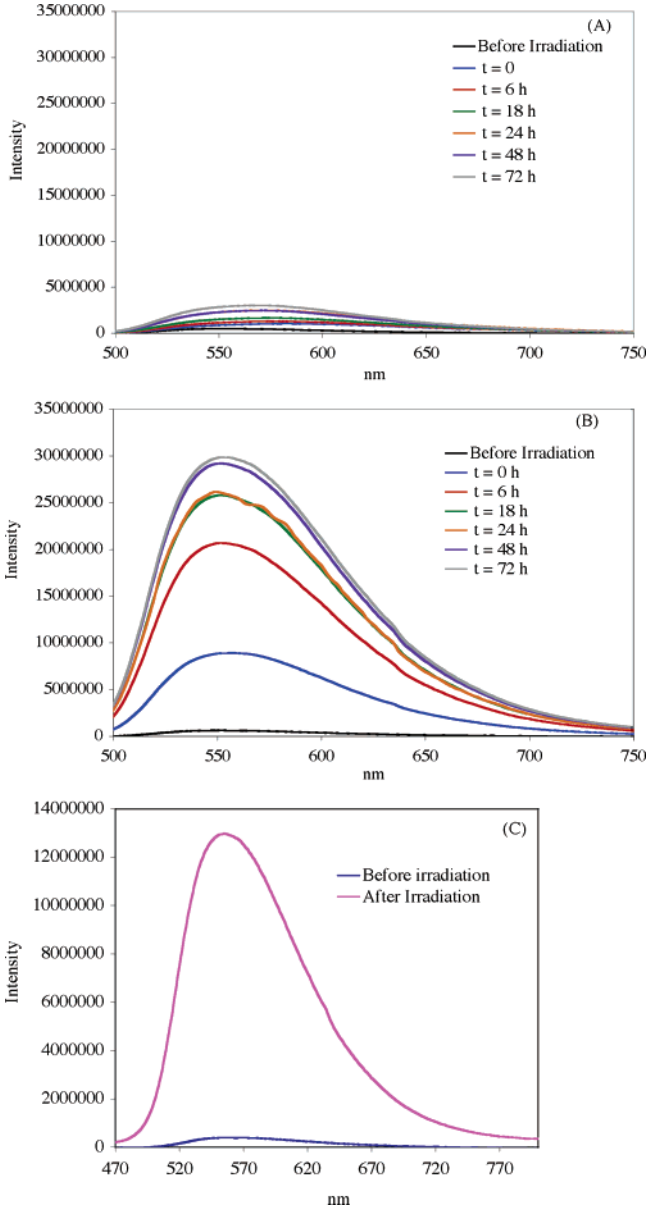

Figure 7. Room-temperature emission spectra of **2** and **2a** in CH_2Cl_2 recorded during a photostability study with broad-spectrum irradiation (300−700 nm): (A) complex **2** in anhydrous CH_2Cl_2, (B) complex **2** in wet CH_2Cl_2, (C) complex **2a** in wet CH_2Cl_2.

(87) Scaiano, J. C. *CRC Handbook of Organic Photochemistry*; CRC Press: Boca Raton, FL, 1989.

In the case of the amine dyad **2a**, similar evidence of photoinstability was obtained. Immediately after **2a** was irradiated for 1 h in *wet* CH_2Cl_2 with visible light, a marked decrease in the absorbance band at 400 nm was seen (Figure S7C), and the emission maximum was seen to exhibit a great increase in intensity with an immediate blue shift of the emission maximum to a value similar to that of the parent chromophore **1** (Figure 7C).

Photohydrolysis has been observed previously in solutions of metal complexes.[88−92] Based on these reports, it is believed that, for the imine-linked dyads, the formation of **1** proceeds through an iminium ion generated upon photoinduced electron transfer from the donor to the Pt metal center, followed by reaction with H_2O. For the amine-linked dyads, the same reaction manifold is accessible following initial arylamine oxidation followed by proton loss and subsequent electron and proton loss steps to generate the corresponding imine. Because the instability of the complexes was observed *only* under photolytic conditions in contrast to samples that exhibited stability in the dark, we conclude that the observed decomposition reaction is a photochemically driven hydrolysis process.

Conclusions

The present work describes the use of Schiff base condensation as a means of generating new Pt(diimine)bis(acetylide)-based donor−chromophore (D−C) dyads. The parent aldehyde, $Pt(dpphen)(C{\equiv}CC_6H_4CHO)_2$ (**1**), is brightly luminescent with a long-lived excited state in CH_2Cl_2 (3 μs), whereas emission of the corresponding D−C dyads is effectively quenched by the attached aniline donors in all solvents tested. The dyad complexes exhibit a dpphen-based reversible one-electron reduction and an irreversible oxidation of the attached aniline donors. Complexes **2** and **2a** display an intense absorption around 400 nm that is shown to be a $\pi-\pi^*$ transition localized on the highly conjugated ligand system, whereas all other dyads exhibit the expected $Pt \rightarrow \pi^*$(dpphen) MLCT transitions. Although the synthesis of the imine and the corresponding amine dyads **2**/**2a**−**4**/**4a** is facile, irradiation experiments of the D−C dyads using a broad spectrum of visible light suggest that both the imine and the amine linkages are highly susceptible to photohydrolysis. This difficulty essentially makes this approach undesirable for further development in the construction of systems for photoinduced charge separation.

Acknowledgment. We thank the Department of Energy, Division of Chemical Sciences, for support of this research and Ms. Christine Flaschenreim for assistance with structural aspects of this study.

Supporting Information Available: Crystal data, atomic coordinates, bond distances, bond angles, and anisotropic displacement parameters for **1**−**4** and **4a** in CIF format. ORTEP diagrams of complexes **3** and **4**, absorption spectra of complexes **3**/**3a** and **4**/**4a** in different solvents, and emission spectra of **1**, **3**, and **4** in different solvents. This material is available free of charge via the Internet at http://pubs.acs.org.

IC048886L

(88) DeLaive, P. J.; Foreman, T. K.; Giannotti, C.; Whitten, D. G. *J. Am. Chem. Soc.* **1980**, *102*, 5627−5631.
(89) Wang, Y.; Hauser, B. T.; Rooney, M. M.; Burton, R. D.; Schanze, K. S. *J. Am. Chem. Soc.* **1993**, *115*, 5675−5683.
(90) Lucia, L. A.; Wang, Y.; Nafisi, K.; Netzel, T. L.; Schanze, K. S. *J. Phys. Chem.* **1995**, *99* (31), 11801−11804.
(91) Lucia, L. A.; Whitten, D. G.; Schanze, K. S. *J. Am. Chem. Soc.* **1996**, *118* (12), 3057−3058.
(92) Wang, Y.; Schanze, K. S. *J. Phys. Chem.* **1996**, *100*, 5408−5419.